ANALYSIS OF THE BURST TEST GEOMETRY A NEW APPROACH

John C. Strikwerda
Associate Professor
Computer Sciences Department
University of Wisconsin-Madison

John M. Considine
Research General Engineer
U.S.D.A. Forest Service
Forest Products Laboratory
Madison, WI 53705

ABSTRACT

The burst or Mullen test is used extensively by the paper industry as a quality assurance tool, however a thorough analysis of this test method is lacking. This report provides information on previous burst test analyses and gives the details of a new analysis. The new analysis, based on membrane theory, allows unlimited deformation and no shape specification for the deformation. This theory is applicable when the deformation of the specimen is greater than the specimen thickness. This theory does not include bending effects, which is reasonable in most paper applications.

Keywords: membrane, burst test, burst strength, numerical methods.

INTRODUCTION

The burst or Mullen test is used throughout the paper, paperboard, and corrugated paperboard industries as a measure of product integrity. The test has achieved wide acceptance because it is fast, easy to perform, and provides a measure of product acceptability. Converters of paper and paperboard often include burst test results in their purchase contracts. The packaging industry manufactures boxes to meet burst specifications.

In the burst test, a paper specimen is clamped by circular, rigid clamps and loaded by a rubber diaphragm, which in turn is displaced by a fluid. The pressure causing the specimen to rupture is called the burst factor. This test was designed to simulate a papermaker's old test of paper, where the papermaker would hold a sheet of paper and try to puncture the paper with their thumb (1).

Other researchers have analyzed the burst test geometry by one of two methods. The first method assumes a spherical deformation from which stresses can be determined. The second method is an extension of von Karman plate theory to nonlinear orthotropic materials. This method is limited to a maximum deflection on the order of the specimen thickness. These theories have proved inadequate for predicting burst behavior of paper because the shape is not spherical and the deflection is very large compared to the thickness. This paper provides an alternative analysis which imposes no limitation on the shape of deformation or the material constitutive behavior. The sole limitation of this analysis is that bending effects are negligible.

BACKGROUND

Early work in the investigation of burst behavior assumed the shape of the deformed surface was a spherical cap (2-4). This shape was used because it simplified the analysis and seemed reasonable based on previous work (5). By assuming this shape and also assuming that paper is a linear elastic, orthotropic material, these researchers (2-4) related the burst strength to the machine-direction (MD) uniaxial tensile failure strain.

Recently, Suhling (6) has found that the shape of the burst deformation of a paperboard specimen is not spherical, but more nearly parabolic. His analysis used a form of von Karman plate theory for nonlinear orthotropic materials. The system of partial differential equations was solved using the finite element numerical analysis technique. Suhling found that the contribution of bending was negligible; the dominant effect. was due to membrane forces.

Suhling has used the von Karman plate theory to analyze paperboard sheets undergoing cylindrical deformation (7) and paperboard sheets under in-plane loading (8). His small deformation results agree with experimental measurements of the out-of-plane deformations.

Experimental investigation of the burst test has found that basis weight, sheet densification and degree of pulp refinement affect the burst strength (9, 10). In addition, Johnson et al. (11) have listed several other papermaking variables which affect burst strength, such as, specimen thickness, formation, sizing, 2-sidedness, and mechanical properties and bondedness of the fibers of the paper. Because the burst results depend on so many variables, the burst strength is not an intrinsic material property.

Careful procedures are required to perform a burst test. Too high or too low clamping pressures produce erroneous results (12-14); test room relative humidity should be carefully controlled (15, 16); rubber diaphragms should be kept in good condition and replaced periodically.

The burst test geometry produces a biaxial stress state in the paper. Scientists have measured the biaxial strength of paper (17, 18) and found that the biaxial tensile strength of paper usually exceeds the uniaxial tensile strength of paper. Suhling et al. (19) have used tensorial failure theories to predict the failure of paperboard experiencing biaxial stress. Use of this result requires a biaxial strength test.

MEMBRANE ANALYSIS

Derivation of the equations for membrane behavior have been presented (20, 21), however, an alternative derivation is provided here to reveal assumptions and limitations of membrane theory.

Consider an undeformed two-dimensional body, Ω, and the deformed body, $\Psi(\Omega)$, which is the result of mapping Ψ from Ω into R^3. The deformation gradient tensor, F, is defined as

$$F = \vec{\nabla}\Psi .$$

Using polar coordinates (ρ, ϕ) on the disk Ω and cylindrical coordinates in R^3, we have $\Psi(\rho,\phi) = (r(\rho,\phi), \theta(\rho,\phi), z(\rho,\phi))^T$. Then

$$F = \begin{pmatrix} \frac{\partial r}{\partial \rho} & \frac{1}{\rho}\frac{\partial r}{\partial \varphi} \\ r\frac{\partial \theta}{\partial \rho} & \frac{r}{\rho}\frac{\partial \theta}{\partial \varphi} \\ \frac{\partial z}{\partial \rho} & \frac{1}{\rho}\frac{\partial z}{\partial \varphi} \end{pmatrix}$$

The Jacobian for the transformation is the square root of the determinant of $F^T F$, i.e.,

$$J = \det(F^T F)^{1/2} .$$

The unit, normal to the surface $\Psi(\Omega)$ at $\Psi(\rho,\phi)$, $\vec{m}$, is the cross-product of the two columns of F, normalized to unit length. So,

$$\vec{m} = \begin{pmatrix} m_1 \\ m_2 \\ m_3 \end{pmatrix} = \begin{pmatrix} \frac{\partial \theta}{\partial \rho}\frac{\partial z}{\partial \varphi} - \frac{\partial z}{\partial \rho}\frac{\partial \theta}{\partial \varphi} \\ \frac{1}{r}(\frac{\partial z}{\partial \rho}\frac{\partial r}{\partial \varphi} - \frac{\partial r}{\partial \rho}\frac{\partial z}{\partial \varphi}) \\ \frac{\partial r}{\partial \rho}\frac{\partial \theta}{\partial \varphi} - \frac{\partial \theta}{\partial \rho}\frac{\partial r}{\partial \varphi} \end{pmatrix} \frac{1}{M}$$

where M is the positive scalar which normalizes $\vec{m}$ to have unit length.

To derive the equations describing the deformation of the membrane, we consider a small subdomain P of Ω. The deformed membrane contains the subdomain $\Psi(P)$ and we assume that the boundary transform nicely, i.e., $\partial\Psi(P) = \Psi(\partial P)$. At a point q in $\partial\Psi(P)$ the outer normal to $\partial\Psi(P)$ in the tangent plane to $\Psi(\partial P)$ will be denoted $\vec{\eta}$. If $\vec{\tau}$ is the unit tangent vector to $\partial\Psi(P)$, then $\vec{m} = \vec{\eta} \times \vec{\tau}$, assuming the usual orientations.

We now consider the static force balance on the membrane. This is simply the balance between the pressure force and the force due to stretching of the materials on each portion. Mathematically this is expressed as

$$\int_{\Psi(P)} p_0 \vec{m} da = \int_{\partial\Psi(P)} T \cdot \vec{\eta} d\ell$$

where p_0 is the constant applied pressure per unit area, T is the stress tensor, ℓ is the arc length along $\partial\Psi(P)$. Notice that because membrane theory assumes negligible thickness, the stress tensor has units of force per unit length.

Our first form of the force balance equation comes from applying the divergence theorem to the above equation. We obtain

$$-\int_{\Psi(P)} p_0 \vec{m} da = \int_{\Psi(P)} div(T) da$$

and since P is an arbitrary domain,

$$-p_0 \vec{m} = div(T) .$$

Together with a constitutive relation, expressing T as a function of F, and other quantities, the above equation describes the deformation of the membrane under the pressure force.

From a computational standpoint the above equation is unsatisfactory since the divergence operator is defined in terms of the unknown surface. We now reformulate the problem to use derivatives on the undeformed region. This is essentially a change of variables in the integrals.

By definition of the Jacobian we have

$$\int_{\Psi(P)} \vec{m}\, da = \int_P \vec{m} J\, dA$$

using dA as the measure of area on P. Also,

$$\int_{\partial\Psi(P)} T \cdot \vec{\eta}\, d\ell = \int_{\partial P} TG \cdot \vec{n}\, dL$$

where $\vec{n}$ is the outer unit normal on ∂P,

$$G = F(F^T F)^{-1} J,$$

and L is arc length on ∂P. Applying the divergence theorem on P we have

$$-p_0 \int_P \vec{m}\, J dA = \int_P DIV(TG) dA$$

giving the equation

$$-p_0 \vec{m} J = DIV(TG) . \tag{1}$$

We use the notation of Gurtin (22) to distinguish the divergence operator *div* on the deformed membrane and the divergence operator *DIV* on the undeformed membrane. The above equation is a nonlinear partial differential equation for the position vector of the deformed membrane as a function of its position in the undeformed membrane. It expresses the balance between the normal pressure force and the stresses within the membrane.

To solve equation (1), the constitutive relation relating T to the displacement must be specified. First, the invariance under observer changes, see (22), shows that T must have the form

$$T = F\tilde{T}F^T$$

where $\tilde{T}$ is a function of only $F^T F$. Moreover, since there are no stresses when there is no strain, $\tilde{T}(I) = 0$. Writing $S = TG$, we have

$$S = TG = F\tilde{T}F^T F(F^T F)^{-1} J = F\tilde{T}J.$$

More than this, little can be said about the constitutive relation. For deviations that are not too large we can expand $\tilde{T}$ in a Taylor series about the state of no deformation. We have that $\tilde{T}$ can be expanded as a a linear matrix-valued function of $F^T F - I$ plus higher-order terms in $F^T F - I$. However, a linear isotropic matrix-valued function mapping square $n \times n$ matrices to $n \times n$ matrices is necessarily of the form

$$L(X) = 2\mu X + \lambda \mathrm{tr}(X) I,$$

for some constants μ and λ, see (22). For the rest of this paper we restrict restrict to the case of isotropic membranes with deflections that are relatively small, thus we may take

$$\tilde{T} = 2\mu(F^T F - I) + \lambda I\ \mathrm{tr}(F^T F - I).$$

AXISYMMETRIC ANALYSIS

As a first attempt at solving equation (1), we make the assumption that the solution is axisymmetric. This assumption is certainly allowable for isotropic materials. Joshi and Murphy (20) have argued that compatibility equations from differential geometry require that the deformation be axisymmetric. (They assumed that one of the lines of principle curvature was a plane curve.) The system of differential equations in equation (1) become

$$-p_0 J m_1 = \frac{1}{\rho}\frac{\partial}{\partial\rho}(\rho S_{11}) - \frac{1}{\rho}S_{22} \tag{2}$$

$$-p_0 J m_3 = \frac{1}{\rho}\frac{\partial}{\partial\rho}(\rho S_{31}) . \tag{3}$$

The assumption of axisymmetric behavior is further justified by the experimental work of Suhling (7), who showed using the optical technique of shadow moire, that the deformation for a paper specimen in the burst test geometry is axisymmetric. Lekhnitskii (23) developed an analytic solution which was axisymmetric for the case of a anisotropic circular plate under uniform pressure loading with clamped edges. We plan further numerical analysis of the generalized system of equation to examine the axisymmetry of this problem.

NUMERICAL SOLUTION

While equations (2) and (3) are very simplified from equation (1), an analytic solution probably does not exist, therefore numerical solution of these equations is required.

The finite difference technique offers unique advantages for solving these equations as compared to the finite element method. Finite difference programs are generally smaller and written for specific applications whereas finite element programs are usually very large and engineers generally use commercial programs. Because the shape of the boundary for this problem is regular and smooth, accurate solutions can be obtained with as few as 5 difference points in the radial direction.

The partial differential equations (2) and (3) were approximated by the following finite difference scheme. Equation (2) was approximated as

$$-p_0 J_i m_{1,i} = \frac{1}{\rho_i}\left(\rho_{i+1/2}S_{11,i+1/2} - \rho_{i-1/2}S_{11,i-1/2}\right)/\Delta\rho - \frac{1}{\rho_i}\left(S_{22,i+1/2} + S_{22,i-1/2}\right)/2 \tag{4}$$

and equation (3) was approximated as

$$-p_0 J_i m_{3,i} = \frac{1}{\rho_i}\left(\rho_{i+1/2}S_{31,i+1/2} - \rho_{i-1/2}S_{31,i-1/2}\right)/\Delta\rho \tag{5}$$

The tensor S was computed as

$$S_{i+1/2} = F_{i+1/2}\tilde{T}_{i+1/2}J_{i+1/2}$$

where

$$F_{i+1/2} = \begin{pmatrix} \left.\frac{\partial r}{\partial\rho}\right|_{i+1/2} & 0 \\ 0 & \left.\frac{r}{\rho}\right|_{i+1/2} \\ \left.\frac{\partial z}{\partial\rho}\right|_{i+1/2} & 0 \end{pmatrix}$$

with

$$\left.\frac{\partial r}{\partial\rho}\right|_{i+1/2} = \frac{r_{i+1} - r_i}{\Delta\rho}$$

$$\left.\frac{r}{\rho}\right|_{i+1/2} = \frac{r_{i+1} + r_i}{\rho_{i+1} + \rho_i}$$

and

$$\left.\frac{\partial z}{\partial\rho}\right|_{i+1/2} = \frac{z_{i+1} - z_i}{\Delta\rho}.$$

The tensor $\tilde{T}_{i+1/2}$ was computed as

$$\tilde{T}_{i+1/2} = \mu E_{i+1/2} + \lambda I \operatorname{tr}(E_{i+1/2})$$

where the Euler strain tensor $E_{i+1/2}$ is

$$E_{i+1/2} = \frac{1}{2}(F^T_{i+1/2}F_{i+1/2} - I).$$

The Jacobian $J_{i+1/2}$ is

$$J_{i+1/2} = \det(F^T_{i+1/2}F_{i+1/2})^{1/2} .$$

For the left-hand side of equations (2) and (3) we used

$$J_i = (J_{i+1/2} + J_{i-1/2})/2,$$

and

$$m_i = (m_{i+1/2} + m_{i-1/2})/2,$$

where

$$m_{i+1/2} = \begin{pmatrix} -\left.\frac{\partial z}{\partial\rho}\right|_{i+1/2} \\ 0 \\ \left.\frac{\partial r}{\partial\rho}\right|_{i+1/2} \end{pmatrix} \frac{1}{M_{i+1/2}}$$

with

$$M_{i+1/2} = \left(\left(\left.\frac{\partial z}{\partial\rho}\right|_{i+1/2}\right)^2 + \left(\left.\frac{\partial r}{\partial\rho}\right|_{i+1/2}\right)^2\right)^{1/2} .$$

Notice that second-order accurate differencing and averaging is used throughout.

These equations were solved by a modified successive-over-relaxation method, in which the values of r_i and z_i were updated by multiples of the residuals of the two equations.

If R_i is the residual obtained by subtracting the left-hand side of equation (4) from the right-hand side, and Z_i is obtained similarly from equation (5), then the iterative method can be written as

$$r_i^{k+1} = r_i^k - \omega_1 R_i/(2D_i^3/\Delta\rho^2)$$

$$z_i^{k+1} = z_i^k - \omega_2 Z_i/(2D_i^3/\Delta\rho^2)$$

where

$$D_i = \max\left(\left|\left.\frac{\partial r}{\partial\rho}\right|_{i+1/2}\right|, \left|\left.\frac{\partial r}{\partial\rho}\right|_{i-1/2}\right|, \left|\left.\frac{\partial z}{\partial\rho}\right|_{i+1/2}\right|, \left|\left.\frac{\partial z}{\partial\rho}\right|_{i-1/2}\right|\right)$$

The factor D_i was needed to prevent growth due to nonlinear effects. The choice of iteration parameters, that is ω_1 and ω_2, has a critical effect on the number of iterations necessary for convergence.

COMPUTATIONAL RESULTS

In this section we compare numerical results with the experimental results of Gleyzal (24). Gleyzal subjected a circular, clamped steel membrane to a uniform pressure load.

Figure 1 shows the computed shape of a steel membrane at different pressures. Properties of the steel membrane are:

Elastic Modulus, $\mathcal{E}$ = 207 MPa
Poisson's Ratio, ν = 0.29
Thickness, t = 3.18 mm

We used Hooke's Law, a linear elastic constitutive relation, that is,

$$\tilde{T} = \frac{\mathcal{E}t}{1-\nu^2}((1-\nu)(F^T F - I) + \nu I \operatorname{tr}(F^T F - I))$$

The most important factor in using these equations, illustrated by Figure 1, is that they are applicable when the deformation is very large. In this case, the central deformation is about 3 times the thickness for a pressure of only 345 kPa.

The results shown in Figure 1 agree with the experimental measurement of Gleyzal. At larger pressures, above 1723 kPa, the results are not similar. The plastic deformation of the membrane, not taken into account in this analysis, dominates the deformation at larger pressures.

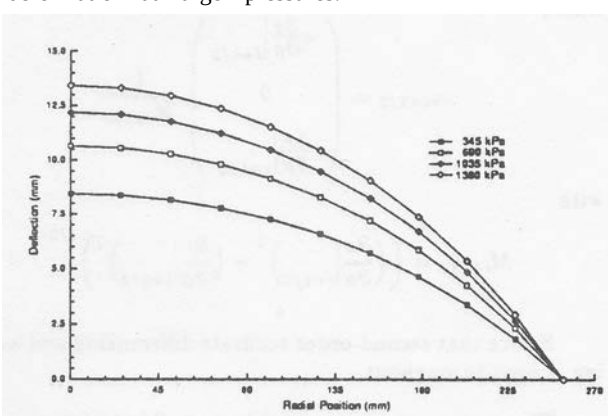

Figure 1. Deformation shapes for various pressures.

Figure 2 shows the effect of pressure on the center deflection of a steel membrane. The figure clearly shows the nonlinear behavior of the equations. Also shown is the fit with a curve giving the deflection proportional to $p_0^{1/3}$. This relation is derived from a perturbation analysis of the system of equations.

Since the behavior of the membrane is axisymmetric, a circle drawn on the undeformed membrane remains a circle on the pressurized membrane. Figure 3 shows the change of radial position of a point at different locations with respect to the undeformed membrane. The abscissa gives the location in the undeformed membrane, and the ordinate gives the change in radial position. Notice that the grid point located at the 152 mm location in the undeformed membrane undergoes the greatest radial displacement. This result is independent of pressure for this case. While the largest strain is at the origin, the largest radial displacement is located midway between the origin and the boundary because the out-of-plane displacement dominates the overall displacement.

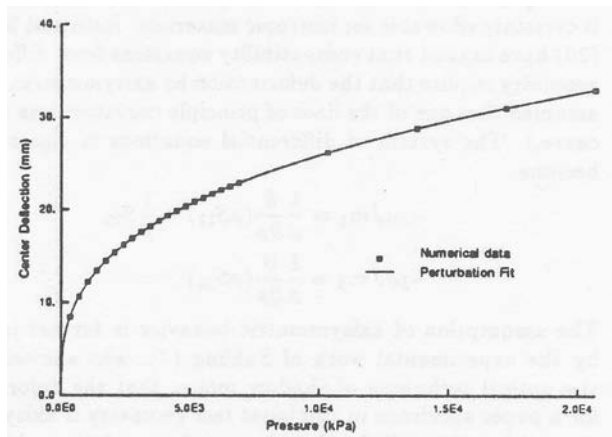

Figure 2. Center deflection versus pressure.

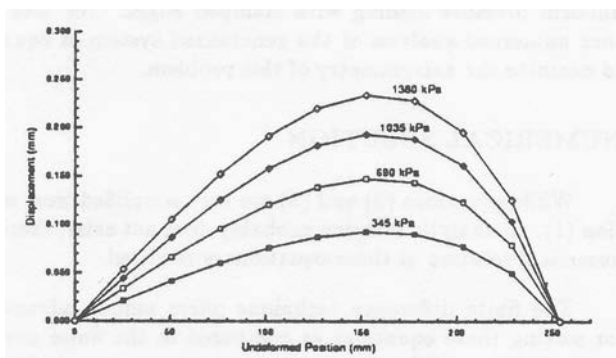

Figure 3. Radial displacement for various pressures.

Richardson extrapolation, or extrapolation to the limit, (25) provides an improved estimate of a calculated value based on the order of accuracy used in the numerical procedure. In this case, we have used second-order accurate finite differences. Table 1 shows the values of the central deflection for 3 grid spacings at 2 pressures. Also shown are the percent deviations from the extrapolated values.

Pressure (kPa)	5 divisions	10 divisions	20 divisions	extra-polated
6,890	22.997 (0.51%)	22.924 (0.19%)	22.890 (0.04%)	22.880
13,780	28.941 (0.46%)	28.849 (0.14%)	28.819 (0.04%)	28.809

Table 1. Center deflection (mm) as a function of grid spacing.

Even for very coarse grids, e.g., 5 divisions, accurate results are achieved. The finer grids may be useful for determining stress and strain at locations in the membrane. Because the

system is elliptic and the scheme is second-order accurate the stress and strain will be second-order accurate (26).

SUMMARY

This paper has presented a derivation of equilibrium equations for the burst test geometry when membrane stresses are dominant. The system of equations were further simplified using axisymmetric arguments and were solved using a finite difference technique.

This technique has advantages over previous burst test analyses, in' that this derivation allows unlimited deformation, any conformable shape, non-uniform but smooth stress distributions, pre-tensioning of the membrane, inhomogeneous material, and any reasonable constitutive behavior.

The results agree with previous experimental work. The numerical procedure can be readily implemented on personal computers.

FUTURE WORK

Several efforts are planned to extend this work. Among them are an analysis of nonlinear, orthotropic paper membranes. This will require the solution of the equations without assuming axisymmetry. A perturbation analysis of the nonlinear system of partial differential equations (1) is in progress. The results of the calculations may provide comparisons with the prediction of failure with several failure theories. It is possible to include effects relating to inhomogeneous materials.

We plan to modify the current approach to analyze the ball burst geometry. The ball burst geometry (27) has been used to more accurately describe material performance in some cases.

REFERENCES

1. Caulfield, D. F. and Gunderson, D. E., "Paper Testing and Strength Characteristics", In: Proceedings of 1988 Paper Preservation Symposium, Washington, DC, October 19–21, 1988, pp. 31-40, 1988.

2. Bohmer, E., "The Analogy Between Burst Testing and Conical Shells", Norsk. Skog. Industri. 16 (9): 382–387, 1962.

3. Van den Akker, J. A., "The Meaning of the Bursting Strength Test", Research Bulletin 4 (3): 46–51, 1938.

4. Stenitzer, F., "Burst Strength", Das Papier 21 (11): 822-828, 1967.

5. Campbell, W. B., "Relation of Bursting to Tensile Tests", Forest Products Labs, Canada, Pulp Paper Lab. Quarterly Rev. 16: 1-4, 1933.

6. Suhling, J. C., "Constitutive Relations and Failure Predictions for Nonlinear Orthotropic Media", Ph.D. Thesis, Mechanics Department, University of Wisconsin-Madison, 1985.

7. Suhling, J. C. "Analysis of Paperboard Deformations Using Nonlinear Plate and Membrane Models", In: Proceedings of the 1987 TAPPI International Paper Physics Conference, Mont-Rolland, Quebec, Canada, September 15–18, 1987, pp. 139–144, 1987.

8. Lin, S. T. and Suhling, J. C., "Supercomputer Analysis of Paperboard Structures", In: Mechanics of Cellulosic and Polymeric Materials, AMD-Vol 99, ed. Perkins, R. W., pp. 113-124, 1989.

9. Bernard, E. and Bouchayer, H., "Manufacturing Parameters Affecting the Characteristics of Corrugating Papers", A. T. I. P. Revue 29 (4): 113–131,1975.

10. Hood, P. F., "Practical Evaluation of Mullen Tests Shows Wide Range of Test Results", Paperboard Packaging, 60 (2): 44-49, 1975.

11. Johnson, J. A., Bennett, K. A., and Montrey, H. M., Chapter 5: Failure Phenomena, In: Handbook of Physical and Mechanical Testing of Paper and Paperboard, ed: Mark, R. E., Vol. 1, Marcel Dekker, Inc., New York, NY, pp. 143–253, 1983.

12. Kill, E. N. and Maltenfort, G. G., "The Effect of Specimen Clamping Pressure on Corrugated Burst Strength", Tappi 57 (11): 67–70, 1974.

13. Aldrich, L. C., "Standardization of Model C Mullen Burst Testers in a Multimill Company", Tappi 43 (5): 221A–225A, 1960.

14. Snyder, L. W., "A Study of the Mullen Paper Tester", Paper Trade Journal, 85 (5): 47-49, 1927.

15. Abrans, A., "A Study of the Mullen Tester on Paperboard", Paper Trade Journal 81 (6): 54–63, 1925.

16. Douty, D. E., "Bursting Strength", Paper Trade Journal 59 (6): 271–276, 1910.

17. deRuvo, A., Carlsson, L., and Fellers, C., "The Biaxial Strength of Paper", Tappi, 53 (5): 133–136, 1980.

18. Gunderson, D. E., Bendtsen, L. A., and Rowlands, R. E., "A Mechanistic Perspective of the Biaxial Strength of Paperboard", Journal of Eng. Mat. and Tech. 108 (1): 135–140, 1986.

19. Suhling, J. C., Rowlands, R. E., Johnson, M. W., and Gunderson, D. E., "Tensorial Strength Analysis of Paperboard", Exp. Mech. 25 (1): 71–84, 1985.

20. Joshi, S. P. and Murphy, L. M., "Large Axisymmetric Deformation of a Laminated Composite Membrane", J. Appl. Mech. 57 (1): 150–157, 1990.

21. Steigmann, D. J. and Pipkin, A. C., "Wrinkling of Pressurized Membranes", J. Appl. Mech. 57 (1): 624–628, 1989.

22. Gurtin, M.E., An Introduction to Continuum Mechanics, Academic Press, New York, 265 pages, 1981,

23. Lekhnitskii, S. G., Anisotropic Plates, 2nd ed., Trans: Tsai, S. W. and Cheron, R., Gordon and Breach Science Publishers, New York, NY, 534 pages, 1968.

24. Gleyzal, A. N., "Plastic Strain and Deflection Tests on Clamped Circular Steel Plates 20 Inches in Diameter", Report R-142, David Taylor Model Basin, Navy Department, 1944.

25. Conte, S. D. and de Boor, C., Elementary Numerical Analysis, An algorithmic approach, 3rd ed., McGraw-Hill Book Company, New York, 432 pages, 1980.

26. Bube, K. P. and Strikwerda, J. C., "Interior Regularity Estimates for Elliptic Systems of Difference Equations", SIAM J. Numer. Anal., 20 (4): 653–670, 1983.

27. Ramasubramanian, M. K. and Ko, Y. C., "Relationship Between the In-Plane Properties and the Ball Burst Strength", In: Mechanics of Cellulosic and Polymeric Materials, ed. Perkins, R. w., AMD-Vol. 99, ASME, New York, NY, pp. 105–112, 1989.

In: Proceedings, 1991 International paper physics conference; 1991 September 22-26; Kona, HI. Atlanta, GA: TAPPI Press; 1991: 579–584. Book 2.

Printed on Recycled Paper